Measurements: The output from detector 1 using cyanoacrylate glue is shown in Fig. 3. Both linear (upper) and logarithmic (lower) time scales are shown. The detected signal evolves through six cycles (12π) before it stabilises, i.e. before the glue is completely cured. The output from detector 2 shows a similar response (not shown), shifted in phase with respect to detector 1. By dissolving the cyanoacrylate with a few drops of dimethyl formamide, the reverse response could be observed with a duration of a few minutes.

The output from detector 1 using epoxy glue is shown in Fig. 4. The spike in the curve is due to a manual interrogation to ensure that the sensor was well adjusted. No induced birefringence could be measured during the full curing time of the epoxy.

Discussion: The measurements in Fig. 3 indicate that the cyanoacrylate glue induces birefringence in optical fibres when used for surface mounting as in Fig. 1. The birefringence is caused by stresses in the fibre core induced during the curing process, with a direction equivalent to that resulting from loading a weight on top of the fibre. The induced birefringence in the fibre is given by the difference in optical path length for the polarisations parallel (n_2) and perpendicular (n_1) to the plate:

$$\frac{2\pi L}{\lambda}(n_1 - n_2) = 12\pi \qquad (1)$$

The birefringence is found to be $B = n_1 - n_2 = 3.6 \times 10^{-5}$. For comparison, the equivalent weight needed to induce the same birefringence may be found using the following formula [7]:

$$B = 4C\frac{f}{\pi r E} \qquad (2)$$

where f is the force per unit length (N/m), $r = 62.5\ \mu m$ is the outer radius of the fibre, and $E = 7.6 \times 10^{10}\ N/m^2$ is Young's modulus for fused silica. The constant C is given as $C = 0.5 \times n_o^3 (p_{12}-p_{11})(1+\nu_p)$, where $n_o = 1.46$ is the average refractive index of the fibre, $p_{11} = 0.113$ and $p_{12} = 0.252$ are the components of the strain-optical tensor of the fibre material [8], and $\nu_p = 0.17$ is the Poisson ratio for the fibre. Taking the measured value of $B = 3.6 \times 10^{-5}$ and inserting numbers into eqn. 2 yields the force needed over 13 cm to produce the same birefringence as gluing with cyanoacrylate as $F = f \times L \simeq 69\,N$. Thus, the cyanoacrylate glue induces a stress in the fibre core equivalent to applying a weight of 7kg on top of the 13cm fibre. This was confirmed experimentally by squeezing the fibre between two glass plates. The required weight to induce a polarimeter readout of 12π was 7.8kg.

There are two reasons for the large difference between the cyanoacrylate and the epoxy. First, the cyanoacrylate shrinks more during the curing process than the epoxy; secondly, by inspection of Fig. 1, it is evident that any shrinking of the thin layer of cyanoacrylate glue will produce an anisotropic stress in the fibre. For the epoxy, the stresses will affect the fibre more uniformly due to the larger volume of epoxy surrounding the fibre. No attempt to distinguish between the two effects has been made.

For a polarimetric sensor consisting of a birefringent fibre, the added birefringence is unwanted. The glue induced birefringence will be superimposed on the internal birefringence of the fibre, which, for example, for bow-tie fibres has axes with arbitrary orientations with respect to the surface. The net sensor response will therefore be disturbed in an unpredictable manner.

For a Bragg grating, the induced birefringence will cause the reflected spectrum for the two polarisations to split. The shift between the two centre wavelengths for the two polarisations for a 1550 nm grating will be given by $\Delta\lambda_b = 2(n_1-n_2)\,\Lambda \simeq 38\,pm$. For a Bragg grating used as a strain sensor the typical strain-wavelength conversion factor is 1.2pm/με at 1550nm [1]. The cyanoacrylate thus causes an increased uncertainty in strain measurements of 32με, which for many applications is unacceptable. Polarisation splitting of Bragg gratings glued using cyanoacrylate of this order and larger has been observed by the authors. In [9], a polarisation splitting of 60pm for a surface mounted Bragg grating using cyanoacrylate glue was reported. Here, the grating was mounted in a v-groove, which further enhances the glue induced stresses.

Conclusions: The birefringence introduced by two commonly used glues for surface mounting optical fibres was investigated. Cyanoacrylate glue was found to induce a birefringence in a standard singlemode optical fibre of 3.6×10^{-5}, which for many sensor applications is unacceptable. A thick layer of epoxy glue induced no measurable birefringence. Hence, if an application requires low fibre birefringence, epoxy is a better choice than cyanoacrylate. Further, for measurements involving cyanoacrylate, the curing time for most commercially available glues is 24h or more.

13 February 1997
Electronics Letters Online No: 19970528

H. Storøy (*Faculty of Electrical Engineering and Computer Science, Norwegian University of Science and Technology, N-7034 Trondheim, Norway*)

K. Johannessen (*SINTEF Department of Electronics and Cybernetics, N-7034 Trondheim, Norway*)

References

1 MOREY, W.W., MELTZ, G., and GLENN, W.H.: 'Fibre optic Bragg grating sensors'. Proc. SPIE-Int. Soc. Opt. Eng., 1990, Vol. 1169, pp. 98–107
2 RASHLEIGH, S.C.: 'Polarimetric sensors: Exploiting the axial stress in high birefringence fibres'. Presented at First Int. Conf. optical fibre sensors, London, UK, 1983, Paper 4.1
3 MOREY, W.W., BALL, G.A., and SINGH, H.: 'Applications of fiber grating sensors'. Proc. SPIE-Int. Soc. Opt. Eng., 1996, **2839**, pp. 2–7
4 HOGG, W.D., TURNER, R.D., and MEASURES, R.M.: 'Polarimetric fibre optic structural strain sensor characterisation'. Proc. SPIE-Int. Soc. Opt. Eng., 1989, **1170**, pp. 542–549
5 NIELSEN, P.L.: 'Investigation of optical fibers as sensors for condition monitoring of composite materials'. Proc. SPIE-Int. Soc. Opt. Eng., 1991, **1588**, pp. 229–240
6 SIRKIS, J.S., and HASLACH, H.W., Jr.: 'Interferometric strain measurement by arbitrarily configured, surface-mounted, optical fibers', *J. Lightwave Technol.*, 1990, **8**, pp. 1497–1503
7 RASHLEIGH, S.C.: 'Origins and control of polarisation effects in single-mode fibers', *J. Lightwave Technol.*, 1983, **1**, pp. 312–331
8 BERTHOLDS, A., and DÄNDLIKER, R.: 'Determination of the individual strain-optic coefficients in single-mode optical fibers', *J. Lightwave Technol.*, 1988, **6**, pp. 17–20
9 HJELME, D.R., BAKKE, B., RAMBECH, J.S., and NEEGÅRD, S.: 'Multiplexed fiber optic Bragg-grating strain sensor system for use in marine vehicle testing'. Proc. SPIE-Int. Soc. Opt. Eng., 1996, Vol. 2838, pp. 40–51

Miniature optical fibre ultrasonic hydrophone using a Fabry-Perot polymer film interferometer

P.C. Beard and T.N. Mills

Indexing terms: Fibre optic sensors, Light interferometers, Hydrophones

An optical fibre hydrophone for the measurement and detection of ultrasound is described. The active sensing element consists of a low finesse Fabry-Perot polymer film interferometer bonded to the tip of an optical fibre, of 50μm core diameter and 0.25mm outer diameter. Sensitivity was found to be 114mV/MPa with an acoustic noise floor of 15kPa over a 25MHz bandwidth.

Introduction: Ultrasonic hydrophones such as those based on piezoelectric PVDF sensing elements are widely used for characterising ultrasound fields [1]. There can, however, be problems associated with the electrical nature of piezoelectric devices, including sensitivity to EMI and cable loading and resonance effects due to the connecting cable. Fragility, expense and the difficulties involved in fabricating small (<100μm) active element diameters for low directional sensitivity whilst retaining adequate acoustic sensitivity can also present limitations. We describe a miniature optical fibre hydrophone which, by its electrically passive nature, small active diameter and simplicity of fabrication, has the potential to overcome these disadvantages. The acoustically active element comprises a thin polymer film (~50μm) acting as a

low finesse Fabry-Perot interferometer [2] mounted at the tip of an optical fibre. An incident acoustic wave modulates the thickness of the film and hence the optical phase difference between the laser light reflected from the two sides of the film. This produces a corresponding intensity modulation of the light reflected from the film. For optimum sensitivity and linearity, the interferometer should be operated at a phase bias that corresponds to quadrature. An advantage of using a polymer film as an extrinsic interferometric acoustic sensing element, rather than the fibre itself [3, 4], is that the low Young's modulus of polymers enables high acoustic sensitivity to be achieved, even when using a sensing film of only a few tens of micrometres thick to obtain a wideband acoustic response at megahertz frequencies.

Theoretical and experimental aspects of this type of optical fibre ultrasound sensor have previously been reported using a large (12 mm) diameter sensor head containing a transparent water-backed sensing film [5]. In this Letter, a miniature (0.25mm) rigid-backed configuration in which the sensing film is bonded directly to the end of the optical fibre is described.

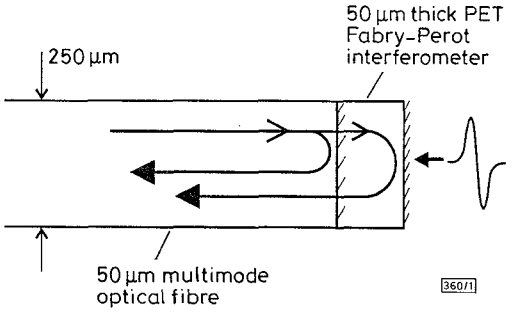

Fig. 1 *Sensor head*

Experiment: The sensor head used is shown schematically in Fig. 1. The optical fibre used was a 50μm core all-silica multimode fibre of numerical aperture 0.1 and outer diameter 0.25mm. The Fabry-Perot polymer sensing film bonded to the cleaved end of the fibre comprised a 0.25mm diameter disk of 50μm thick PET (polyethylene terepthalate) with a 40% optically reflective aluminium coating on one side and a 100% reflective coating on the other; the two coatings form the mirrors of the interferometer. The sensing film was interrogated using 633nm light from a 7mW He Ne laser and the reflected intensity modulation was transmitted back along the fibre for detection at a 25MHz photodiode with an integral transimpedance amplifier. In the absence of a tunable laser source, operation close to quadrature was obtained by a process of trial and error. A number of optical fibre hydrophones were fabricated using sections of PET sensing film cut from different parts of the same sheet. The slight variations in thickness over the area of the polymer film sheet produced a range of different phase biases and hence sensitivities. The optical fibre hydrophone that gave the highest sensitivity was assumed to have a thickness that resulted in a phase bias close to quadrature, and was used for these experiments. The short path length of the polymer film interferometer (100μm) means that, once set at quadrature, the sensor is inherently insensitive to environmental thermal and pressure fluctuations giving good stability [5].

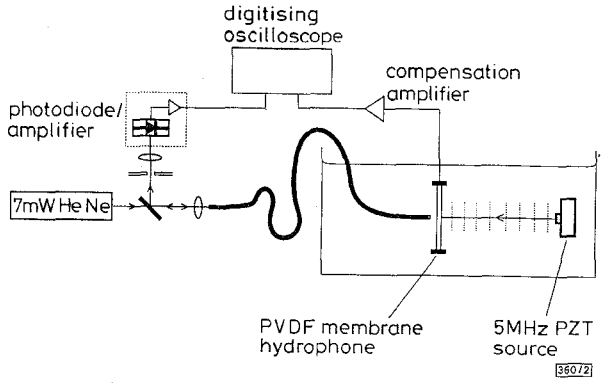

Fig. 2 *Experimental arrangement*

The optical fibre hydrophone was inserted into a water tank and positioned directly behind the active region of a calibrated, 50μm thick, 25MHz bilaminar PVDF membrane reference hydrophone of active diameter of 0.5mm (Fig. 2). A compensation amplifier was used to correct for any small variations in the frequency response of the membrane hydrophone, ensuring a uniform response (to within 1dB) up to 20MHz. Since this type of hydrophone provides minimum perturbation to the acoustic field under measurement, it was assumed not to affect the measurement of the optical fibre hydrophone. A pulsed 5MHz PZT transducer of 13mm diameter was used as the ultrasound source. The separation between the source and hydrophone was ~6cm. A 500MHz digitising oscilloscope was used to capture the waveforms from each device.

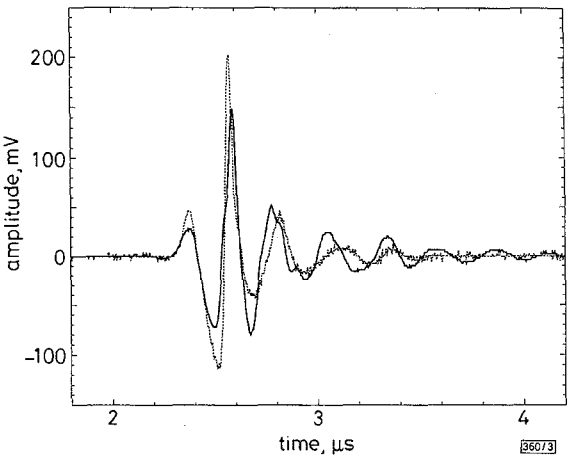

Fig. 3 *Comparison between optical fibre hydrophone output and PVDF membrane hydrophone output in response to 1.3MPa acoustic signal*

——— optical fibre hydrophone output
– – – – PVDF membrane hydrophone output

Results: A comparison between the output of the optical fibre hydrophone and the PVDF membrane hydrophone system is shown in Fig. 3. The sensitivity of the optical fibre hydrophone is 114mV/MPa with an acoustic noise floor of < 15kPa over a 25MHz bandwidth. The corresponding sensitivity and acoustic noise floor of the PVDF membrane hydrophone system is 155mV/MPa and 40kPa, respectively. The sensitivity of the optical fibre hydrophone is almost a factor of 2 higher than that previously reported using a water-backed polymer sensing film [5]. This is because the rigid-backed configuration shown in Fig. 1 produces a higher acoustically-induced strain in the polymer film.

The temporal profiles of the two waveforms shown in Fig. 3 are in good agreement for the first two cycles of the signals. Thereafter, the signals begin to differ in relative amplitude and phase, indicating a non-uniformity in the frequency response of the optical fibre hydrophone. There are several possible reasons for this. (i) the thickness of the optical adhesive used to attach the sensing film to the tip of the fibre is sufficiently large that acoustic reflections from the cleaved end of the fibre are significantly time-delayed; (ii) the sensor is not operating solely in thickness mode and acoustic energy is being coupled into the radial direction causing radial resonance modes to be excited; (iii) diffraction around the tip of the fibre may also be responsible. Additionally, the discrepancy may be due to spatial variations in the acoustic field, the effect of which is related to the differing degrees of spatial integration produced by each device due to their large differences in active diameters.

A measure of the directional response of the optical fibre hydrophone was obtained by altering the angle of the optical fibre to the incident acoustic field and computing the FFT of the output waveforms for three angles. The amplitude component at the 5MHz transducer centre frequency fell by a factor of 1.8 when the fibre was orientated at 45° to the incident field and by a factor of 3.3 at 90°. Despite the large angular increments, this indicates that the optical fibre hydrophone has a sufficient degree of omnidirectionality to provide a useful output even when aligned orthogonally to the acoustic field. Its relatively low directional sensitivity is a consequence of its small active area which, to a first approximation, is defined by the 50μm diameter of the optical fibre output incident on the sensing film.

Conclusion: A miniature ultrasonic optical fibre hydrophone of small active area that has a sensitivity which is comparable to piezoelectric devices has been demonstrated. The frequency response of the system requires further investigation to determine whether the differences in the temporal output between the PVDF membrane hydrophone and the optical hydrophone are due to the experimental setup or are inherent in the design of latter. For practical use a tunable laser diode could be used to obtain quadrature on 'start-up' and maintain it thereafter. It is envisaged that this system has the potential for use in characterising the output of ultrasonic transducers and as a general purpose tool for the measurement and detection of ultrasound. A particular application is the *in vivo* safety-related exposure measurements of the output of diagnostic and therapeutic medical ultrasound equipment. Such an application would benefit from the small physical size, omnidirectionality, and electrical passivity that this technology has the potential to offer.

Acknowledgements: The authors would like to thank F. Duck of the Royal United Hospital Bath for his help in making the measurements described above and A. Coleman of St Thomas's Hospital, London for his assistance throughout this project. This work was originally funded by the MRC and is currently supported under the DTI/EPSRC LINK Photonics scheme in collaboration with Precision Acoustics Ltd, Dorchester, Dorset.

20 February 1997
Electronics Letters Online No: 19970545

P.C. Beard and T.N. Mills (*University College London, Department of Medical Physics and Bioengineering, Shropshire House, 11-20 Capper Street, London WC1E 6JA, United Kingdom*)

References

1 LEWIN, P.A.: 'Practical implementations and technology of measurement devices', *in* ZISKIN, M.C., and LEWIN, P.A. (Eds.): 'Ultrasonic exposimetry' (CRC Press, Boca Raton, USA, 1993), Chap. 7, pp. 189–197
2 BEARD, P.C., and MILLS, T.N.: 'An optical fibre sensor for the detection of laser generated ultrasound in arterial tissues', *Proc. SPIE - Int. Soc. Opt. Eng.*, 1994, **2331**, pp. 112–122
3 ALCOZ, J.J., LEE, C.E., and TAYLOR, H.F.: 'Embedded fibre-optic Fabry-Perot ultrasound sensor', *IEEE Trans. Ultrason., Ferroelectr. Freq. Control*, 1990, **37**, (4), pp. 302–305
4 DORIGHI, J.F., KRISHNASWAMY, S., and ACHENBACH, J.D.: 'Stabilisation of an embedded fibre optic Fabry-Perot sensor for ultrasound detection', *IEEE Trans. Ultrason., Ferroelectr. Freq. Control*, 1995, **42**, (5), pp. 820–824
5 BEARD, P.C., and MILLS, T.N.: 'Extrinsic optical fibre ultrasound sensor using a thin polymer film as a low finesse Fabry-Perot interferometer', *Appl. Opt.*, 1996, **35**, (4), pp. 663–675

Optical add/drop multiplexer based on UV-written Bragg grating in a fused 100% coupler

F. Bakhti, P. Sansonetti, C. Sinet, L. Gasca,
L. Martineau, S. Lacroix, X. Daxhelet and F. Gonthier

Indexing terms: Gratings in fibres, Optical couplers, Multiplexing

The authors report the first realisation of a simple and stable optical add/drop multiplexer based on a UV-written Bragg grating in the coupling region of a fused 100% coupler. Add/drop functions are demonstrated with a low insertion loss (<1dB).

Introduction: The photosensivity occurring in germanium-doped silica under UV irradiation [1] allows the direct and simple realisation of grating filters in optical fibres, with low insertion loss and the potential for low cost. Among them the optical add/drop multiplexer (OADM) is a key component for future WDM networks. A solution based on gratings in a fibre Mach-Zehnder has been demonstrated [2 – 4]. However, these structures require several UV-writing steps to properly balance the gratings and the phases in both arms. Other designs have been proposed based on grating writing in the coupling region [5, 6] of polished fibre couplers, but they do not represent a satisfactory solution to producing compact, stable, and low cost components.

We propose here a breakthrough in OADM technology. Using fused coupler technology, an OADM is developed which is based on a 100% coupler (launched light entirely exits in crossed port) where a strong grating is UV-written in the coupling region. This novel lowloss component offers simple implementation, a compact device, as well as stable operation, since it is based on the interference between two modes in the same guiding region, compared to the Mach-Zehnder configuration where the two arms are separated.

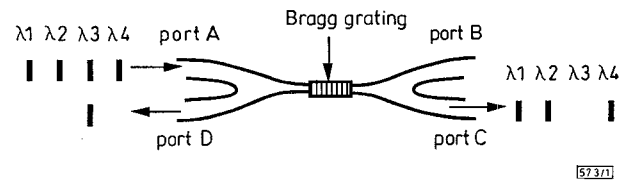

Fig. 1 *Schematic diagram of OADM based on Bragg grating in fused 100% coupler*

Principle of operation: A grating is UV-written in the middle of the coupling region of a 100% coupler (Fig. 1). Light launched in port A is dropped in port D when reflected by the grating, while it exits at port C if it is not.

OADM implementation: Because of the diameter reduction in the coupling region, the grating coupling efficiency is small when standard singlemode fibre is used. We thus fabricated a special fibre with an index profile close to that of standard fibre, but designed with a portion of the cladding made highly photosensitive, but still with a matched cladding configuration, for efficient coupling. 100% lossless couplers could then be manufactured [7] taking into account the lower softening temperature of this fibre, as well as dopant diffusion.

Extinction between the output ports of up to 25dB could be obtained. Couplers were then hydrogen soaked at 150 bar and ambient temperature for 3 days, the time necessary for hydrogen to diffuse into the whole coupling region.

Bragg gratings were then written in the coupling region of the fused couplers, using an excimer pumped dye laser with fluence 80mJ/cm²/pulse.

Experimental results: Resulting performances were measured using a tunable laser launched either in port A to study the drop properties, or in port B for the add properties. Two devices are reported.

A flat-top drop filter with a 1dB insertion loss, measured by cutback techniques, and 20dB transmitted channel extinction at the Bragg wavelength was achieved, resulting from a 8mm long grating written on one side of the coupling region of a 100% coupler (Fig. 2). This filter was not phase matched for the add function, but the result highlights the potential for high extinction bandpass filters, with a stable configuration.

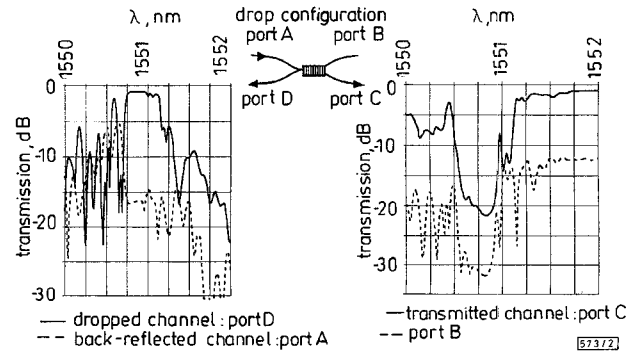

Fig. 2 *Flat-top drop filter achieved by UV-writing 8 mm long grating in coupling region of 100% coupler*

1dB insertion loss, 20dB extinction in transmitted channel C
0.4nm –1dB dropped bandwidth were obtained